The average $\langle \log \tau \rangle$ for the fast relaxation process, as shown in Figure 4, is rather insensitive to T_g variation and is less sensitive to temperature variation than the relaxation time of the slow mode, in agreement with dielectric and mechanical relaxation findings.[11,19] An Arrhenius temperature dependence is therefore more appropriate than the free volume equation, (5). Moreover, the presence of the fast mode in PMMA is consistent with the dielectric relaxation process assigned to the hindered rotation of the $COOCH_3$ side group around the C–C bond linking it to the main chain.[19] The dielectric relaxation time $1/(2\pi f_m)$, where f_m is the frequency at the loss permitivity maximum in the high MW PMMA[19] is also plotted in Figure 4 for comparison. Within experimental uncertainty the temperature dependence of the fast light scattering time is compatible with that obtained in the dielectric relaxation. For the latter, the reported Arrhenius activation energy E is 18 kcal/mol.[19] However, we still need to explain why the relaxation times measured in the high MW PMMA at high temperatures exceed the values obtained from the extrapolation of the low MW data by using E = 18 kcal/mol. We attribute this discrepancy to the cutoff effects present in the ILT analysis. This is probably due to the lack of the short-time plateau in the time correlation functions of high MW PMMA.[7] As a matter of fact, to ascertain the influence of the cutoff effect is one of the reasons for initiating the present investigation.

Conclusion

In this work, we present further convincing evidence for the presence of two relaxation modes in the time correlation functions of PMMA near and above T_g. The retardation spectrum obtained by using the inverse Laplace transform analysis reveals a two-peak structure, although the corresponding time correlation function for the low MW sample (T_g = 52 °C) does not show a clear kink like that observed in the high MW material (T_g = 107 °C) below 128 °C. The long-time peak associated with the primary glass–rubber relaxation displays a strong temperature dependence and the relaxation time versus temperature data are well represented by the VFTH free volume equation. Values of various characterizing parameters are similar in the two PMMA's when allowance is made to take into account the difference in T_g. The light scattering and ultrasonic data on the longitudinal density fluctuations over 12 decades in time can also be fitted to the VFTH equation.

The short-time peak in the retardation spectrum, $L(\log \tau)$ is insensitive to T_g and also displays weaker temperature dependence than the long-time peak. The relaxation times of the short-time peak compare favorably with dielectric data associated with the secondary β-relaxation. In the dynamic range of the currently available correlator, the two relaxation processes are better resolved in the high MW PMMA.

Registry No. PMMA, 9011-14-7.

References and Notes

(1) See, for example: Patterson, G. D. *Adv. Polym. Sci.* **1983**, *48*, 125. Fytas, G.; Wang, C. H.; Meier, G.; Fischer, E. W. *Macromolecules* **1985**, *18*, 1492.
(2) Fytas G. In *Physical Optics of Dynamics Phenomena and Processes in Macromolecular Systems* Sedlacek, B., Ed.; W. de Gruyter: Berlin, New York, 1985; p 205.
(3) Patterson, G. D.; Carroll, D. J.; Stevens, J. R. *J. Polym. Sci., Polym. Phys. Ed.* **1983**, *17*, 613.
(4) Wang, C. H.; Fytas, G.; Lilge, D.; Dorfmüller, Th. *Macromolecules* **1981**, *14*, 1363.
(5) Wang, C. H.; Fischer, E. W. *J. Chem. Phys.* **1985**, *82*, 632.
(6) Wang, C. H.; Fytas, G.; Fisher, E. W. *J. Chem. Phys.* **1985**, *82*, 4332.
(7) Fytas, G.; Wang, C. H.; Fisher, E. W.; Mehler, K. *J. Polym. Sci., Polym. Phys. Ed.* **1986**, *24*, 1859.
(8) Meier, G.; Fytas, G.; Dorfmüller, Th. *Macromolecules* **1984**, *17*, 957.
(9) Lee, M.; Ferguson, R.; Jamieson, A. M.; Simha, R.; Cowie, J. M. G. *Polym. Commun.* **1985**, *26*, 66.
(10) Provencer, S. W. *Comput. Phys. Commun.* **1982**, *27*, 213, 229.
(11) Ferry, J. D. *Viscoelastic Properties of Polymers*; Wiley: New York, 1980.
(12) Koppelmann, J. In *Physics of Noncrystalline Solids*; Prins, J. A., Ed.; North Holland: Amsterdam, 1965; p 255.
(13) Plazek, D. J.; Tan, V.; O'Rourke, V. M. *Rheol. Acta* **1974**, *13*, 367.
(14) Miller, A. *Macromolecules* **1978**, *11*, 859.
(15) Fytas, G.; Patkowski, A.; Meier, G.; Dorfmüller, Th. *J. Chem. Phys.* **1984**, *80*, 2214.
(16) Couchman, P. R. *J. Appl. Phys.* **1979**, *50*, 6043.
(17) Kono, R. *J. Phys. Soc. Jpn.* **1960**, *15*, 718.
(18) Li, B. Y.; Jiang, D. Z.; Fytas, G.; Wang, C. H. *Macromolecules* **1986**, *19*, 778.
(19) Tetsutani, T.; Kakizaki, M.; Hideshima, T. *Polym. J.* **1982**, *14*, 305.

Relaxation Times of Polymer Solutions in the Semidilute Region for Zero-Shear Viscosity

Yoshiaki Takahashi,* Masanari Umeda,† and Ichiro Noda

Department of Synthetic Chemistry, Nagoya University, Furo-cho, Chikusa-ku, Nagoya 464, Japan. *Received June 30, 1987; Revised Manuscript Received January 15, 1988*

ABSTRACT: Relaxation times τ_w and τ_0 of polymer solutions in the semidilute region for the zero-shear viscosity $\eta°$ were studied in good and Θ solvents. Here, τ_w is the weight-average relaxation time evaluated from the product of $\eta°$ and the steady-state compliance J_e, and τ_0 is the relaxation time specifying shear rate dependence of viscosity. It is found that τ_0 is proportional to τ_w regardless of concentration and solvent power, and the concentration and molecular weight dependences of both relaxation times can be well understood if the semidilute region for $\eta°$ is divided into two regions, i.e., the dilute and entangled regions for J_e.

Introduction

In previous papers[1,2] we studied viscoelastic properties of linear polymer solutions over a wide range of concentration and presented molecular weight–concentration diagrams for the viscosity at zero-shear rate or the zero-shear viscosity $\eta°$ and for the steady-state compliance J_e, representing energy dissipation and storage processes, respectively. The concentration dependence of $\eta°$ of polymer solutions can be well understood if we take account of semidilute solutions and classify the polymer

†Present address: Tokai Rubber Industries Ltd., 3600 Utazu, Kitatoyama, Komaki 485, Japan.

0024-9297/88/2221-2257$01.50/0

solutions into three concentration regions, that is, dilute, semidilute, and concentrated solutions. To discuss viscosity data in various concentration regions we define the reduced form of zero-shear viscosity η°_R by

$$\eta^\circ_R = \eta^\circ_{sp}/C[\eta]$$

where $\eta^\circ_{sp} = (\eta^\circ - \eta_s)/\eta_s$, C is the concentration, and $[\eta]$ and η_s are the intrinsic and solvent viscosities, respectively.

In the semidilute solutions, if we assume that the scaling law is applicable to the zero-shear viscosity,[3,4] we would have

$$\eta^\circ_R \propto (C/C^*)^b$$

where $C^* = 3M/(4\pi\langle s^2\rangle^{3/2}N_A)$ is the critical concentration for coil overlapping and $\langle s^2\rangle$ and M are the mean square radius of gyration and the molecular weight of the polymer, respectively. The exponent b can be determined by the molecular weight dependence of η°, $\eta^\circ \propto M^a$ in semidilute solution. In the original work of de Gennes,[3,4] the exponent a was assumed to be 3 according to the reptation model but the experimental value is 3.4. If we assume the experimental value of 3.4 for a, we have

$$\eta^\circ_R \propto (C/C^*)^{(4.4-3\nu)/(3\nu-1)} \quad (1)$$

where ν is an excluded-volume exponent defined as $\langle s^2\rangle \propto M^{2\nu}$. The viscosity behavior in good and Θ solvents in semidilute solutions can be well expressed by eq 1. Since η°_R can be expressed by an expansion form of C/C^* in dilute solutions, the crossover from dilute to semidilute solutions for η° in good solvents occurs at a certain degree of coil overlapping, $C/C^* \simeq 10$, which is much larger than that for thermodynamic properties ($C/C^* \simeq 2$), while the crossover from semidilute to concentrated solutions for η° in good solvents takes place almost at the same concentration as that for thermodynamic properties, say, $C \simeq 0.2$ g/mL, regardless of molecular weight.

In order to understand the concentration dependence of J_e, on the other hand, it is unnecessary to divide an entangled region into semidilute and concentrated solutions by introducing a scaling theory, in contrast to the case of η°. The crossover from dilute to entangled regions occurs at a critical concentration C_c^J determined by the condition that $C_c^J M$ = constant ($\simeq 1.4 \times 10^5$) regardless of solvent power. In dilute solutions, i.e., $C < C_c^J$, J_e is proportional to molecular weight, while in entangled regions, i.e., $C > C_c^J$, J_e is independent of molecular weight:

$$J_e \propto M/C \qquad (C < C_c^J) \quad (2a)$$

$$J_e \propto C^{-a} \qquad (C > C_c^J) \quad (2b)$$

where the values of a are 2.1 in a good solvent and 2.3 in a poor solvent which is close to the Θ condition. The values are different from the exponents predicted by the scaling theory, i.e., 2.27 ($\nu = 0.59_5$) in a good solvent and 2.69 ($\nu = 0.53$) in a poor solvent, but they may be closer to the value (2.0) predicted from the uniform network model irrespective of solvent power.

Moreover, if we compare the crossover concentration from dilute to semidilute regions for η° with that from dilute to entangled regions for J_e at the same molecular weight, the latter is 4–6 times higher than the former. Thus, there is no straightforward relationship between concentration regions for η° and J_e of polymer solutions.

According to the phenomenological theory of linear viscoelasticity,[5,6] η° and J_e are expressed in terms of relaxation time τ

$$\eta^\circ = \int_{-\infty}^{\infty} \tau H(\tau)\, d\ln\tau \quad (3)$$

$$J_e = \eta^{\circ -2} \int_{-\infty}^{\infty} \tau^2 H(\tau)\, d\ln\tau \quad (4)$$

where $H(\tau)$ is the relaxation spectrum. Therefore, $\eta^\circ J_e$ gives a mean relaxation time, which is called the weight-average relaxation time τ_w

$$\tau_w = \int_{-\infty}^{\infty} \tau^2 H(\tau)\, d\ln\tau \Big/ \int_{-\infty}^{\infty} \tau H(\tau)\, d\ln\tau \quad (5)$$

Since there are three and two concentration regions for η° and J_e, respectively, as described above, five concentration regions are possible for τ_w in terms of concentration and molecular weight dependences: (I) dilute solutions for both η° and J_e; (II) semidilute solution for η° and dilute solution for J_e; (III) concentrated solution for η° and dilute solution for J_e; (IV) semidilute solution for η° and entangled region for J_e; (V) concentrated solution for η° and entangled region for J_e. Therefore, studies on the concentration and molecular weight dependences of relaxation times in these concentration regions are important for elucidating viscoelastic properties of polymer solutions.

It should be noted that there are some other discussions on the concentration regions of viscoelastic properties of polymer solutions. Graessley[7] also classified polymer solutions in good solvents into five concentration regions to distinguish viscoelastic behaviors. However, the semidilute but not entangled and concentrated but not entangled regions in his paper are included in the dilute solution for η° in the present work. The crossover from the dilute region to the semidilute but not entangled region in his paper corresponds to that from the dilute to semidilute solutions for thermodynamic properties in our work.[3] In our diagram for J_e the dilute solution or unentangled region is not divided into two regions corresponding to Zimm-like and Rouse-like behavior, since our primary interest is the entangled regions for viscoelastic properties.

A relaxation time τ_0 specifying polymer solutions may also be represented by a characteristic time defined as the inverse of the shear rate at the onset of non-Newtonian viscosity. The functional forms of the shear rate dependence and the relaxation time τ_0 have been studied by many researchers.[9-13] Graessley et al.[9] and Sakai et al.[11] showed that the shear rate dependence of viscoelastic properties in highly entangled regions are well understood by classifying the entangled region into two concentration regions, that is, $C < C_c^J$ and $C > C_c^J$, and employing different functional forms of relaxation times in each region. Berry et al.[12] reported that the ratio of viscosity at finite shear rate $\eta(\dot\gamma)$ to η°, $\eta(\dot\gamma)/\eta^\circ$ can be superposed in terms of $\dot\gamma\tau_w$. Thus, similarity between τ_0 and τ_w or the longest relaxation times in behavior and magnitude was revealed in highly entangled systems. In these works, however, they did not take into account the semidilute region for η° so that the concentration dependence of τ_0 was not directly discussed. Moreover, the shear rate dependence in a Θ solvent is not well studied. In this work, therefore, we study concentration and molecular weight dependences of τ_w and τ_0 in both good and Θ solvents in semidilute solutions for η°, i.e., in regions II and IV. Here, τ_0 was determined by $\tau_0 = 1/\dot\gamma_0$, where $\dot\gamma_0$ is the shear rate at which the shear viscosity $\eta(\dot\gamma)$ is equal to $0.8\eta^\circ$ as proposed by Graessley.[14]

It is noted that the concentration dependence of η° in semidilute solutions is clearly explained by the scaling theory, without taking into account the concentration dependence of local frictional coefficients. In concentrated solutions (regions III and V), however, the concentration dependence of η° is partially due to the variation of local frictional coefficient with concentration.

Table I
Molecular Characteristics

sample	$M_w \times 10^{-6}$ [a]	M_w/M_n [a]	sample	$M_w \times 10^{-6}$ [a]	M_w/M_n [a]
F-2000	20.6		F-288	2.89	1.09
F-850	8.42	1.17	F-128	1.26	1.05
F-450	4.48	1.14	F-80	0.775	1.01

[a] Reported values from manufacturer.

Table II
Zero-Shear Viscosity and Steady-State Compliance

sample	solvent	$C \times 10^2$, g/mL	$\eta°$, P	J_e, cm^2/dyn
F-850	DOP	3.31	6.54×10^3	3.83×10^{-3}
		3.03	5.10×10^3	5.38×10^{-3}
		2.67	1.74×10^3	6.14×10^{-3}
		1.77	2.30×10^2	1.31×10^{-2}
		1.27	2.18×10^1	1.87×10^{-2}
F-288	DOP	5.72	6.24×10^3	9.33×10^{-4}
		3.99	9.00×10^2	1.93×10^{-3}
		2.97	1.75×10^2	2.77×10^{-3}
	α-CN	11.3	3.28×10^3	1.53×10^{-4}
		9.87	1.98×10^3	2.19×10^{-4}
		7.63	5.28×10^2	3.72×10^{-4}
		5.90	1.65×10^2	4.26×10^{-4}
		5.21	8.55×10^1	6.02×10^{-4}
		3.50	1.76×10^1	1.24×10^{-3}
F-80	DOP	10.8	3.00×10^3	1.55×10^{-4}
		8.65	9.20×10^2	2.10×10^{-4}
		6.75	2.32×10^2	3.07×10^{-4}
		4.86	4.17×10^1	3.96×10^{-4}

Experimental Section

The polymer samples used were polystyrenes having narrow molecular weight distributions obtained from Toyo Soda Manufacturing Co., Ltd. Their molecular characteristics are listed in Table I. α-Chloronaphthalene (α-CN) and dioctyl phthalate (DOP) were used as good and Θ solvents [$T(\Theta)$ = 22 °C], respectively. The purification methods and the physical properties of these solvents were reported previously.[11,15]

Weighted amounts of sample and solvent were mixed and gently stirred at 50 °C a few times a day until the solution became uniform. Polymer concentrations determined in weight were converted to grams per milliliter by assuming additivity of the specific volumes of polymer and solvent.

The shear rate dependence of shear stress P_{12} and primary normal stress difference $P_{11} - P_{22}$ were measured with a Weissenberg rheogoniometer of type R-17 (Sangamo Controls Ltd.), equipped with a gap-servo system. A cone–plate geometry with 5-cm diameter and 4° cone angle was used. The details and reliability of measurements with the R-17 were reported in previous papers.[16,17] Temperatures of the measurements were 50.0 °C in α-CN and 22.0 °C in DOP with an accuracy of ±0.1 °C. The measurements of DOP solutions were carried out after both the solutions and the cone–plate were kept at higher temperatures than 22.0 °C and then lowered to the experimental temperature.

Results

The shear viscosity $\eta(\dot{\gamma})$ and the apparent steady-state compliance J_s were evaluated from $P_{12}/\dot{\gamma}$ and $(P_{11} - P_{22})/2P_{12}^2$, respectively, extrapolated to zero shear rate. Most of data of $\eta°$ and J_e in the good solvent used here were reported in the previous paper.[2] The data obtained in this work are listed in Table II and plotted in Figure 1. In this figure the viscosity data are expressed in the alternative form of eq 1 as

$$\eta°_{sp}/M^{3.4} \propto C^{3.4/(3\nu-1)} \quad (6)$$

The polystyrene data reported in the previous work are shown by solid lines. The poly(α-methylstyrene) viscosity data in Θ solvents[1] are denoted by the broken line, some of which are shown by half-filled circles for comparison. It can be seen in this figure that $\eta°$ and J_e data in good solvents agree well with the data from the previous work

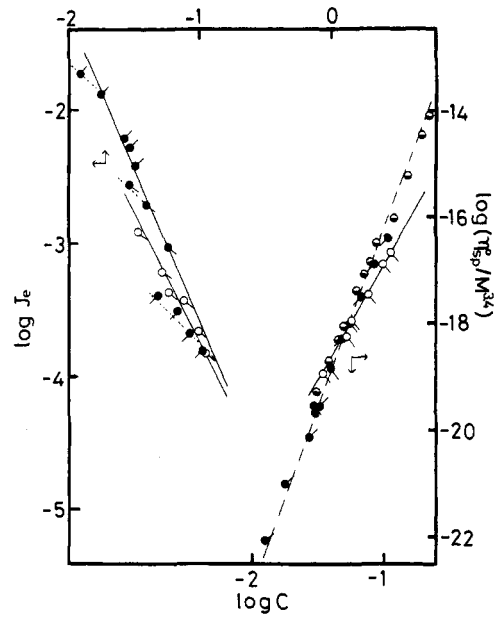

Figure 1. Concentration dependences of J_e and $\eta°_{sp}/M^{3.4}$ for polystyrenes in α-CN and DOP. Symbols (○), (△) and (□) and the corresponding filled circles denote the data for samples F-850, F-288, and F-80 in α-CN and DOP, respectively. Solid lines denote data for polystyrenes in the previous work[2] and half-filled circles denote data for poly(α-methylstyrenes) in Θ solvents.[1]

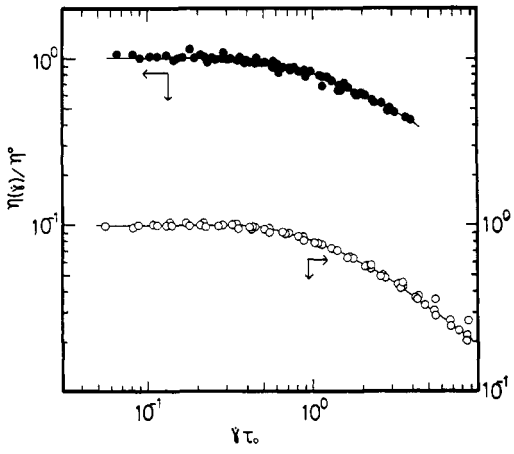

Figure 2. Double-logarithmic plots of $\eta(\dot{\gamma})/\eta°$ versus $\dot{\gamma}\tau_0$ for the samples with various molecular weights over a wide range of concentration in good (○) and Θ (●) solvents.

and also that the $\eta°$ data in the Θ solvent agree with those of poly(α-methylstyrene) in Θ solvents. It is also noted that J_e data in a Θ solvent agree with the data in the poor solvent, which is close to a Θ condition, reported in the previous work. Moreover, it is confirmed by this figure that the concentration ranges of measurements in this work are regions II and IV.

In Figure 2, the shear rate dependence of $\eta(\dot{\gamma})$ of the samples with different molecular weights over a wide range of concentration are shown in the reduced form, log $[\eta(\dot{\gamma})/\eta°]$ versus log $\dot{\gamma}\tau_0$. It is apparent that all data in good and Θ solvents form a single curve for each solvent. Moreover, it is noted that the reduced curves in good and Θ solvents can be superposed with each other and also agree with the data which include regions III and V in the previous papers.[11,13] Thus, it can be concluded that the shear rate dependence of viscosity in the reduced form is independent of solvent power and of concentration region in the entangled regions for viscosity (regions II, III, IV, and V). Moreover, the superposition of the data in terms of τ_0 implies that the relaxation time τ_0 evaluated here is

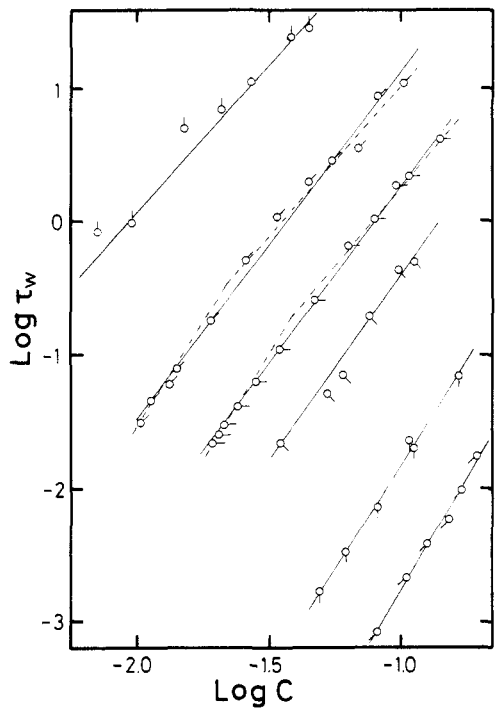

Figure 3. Concentration dependence of τ_w in good solvents. Symbols (♁), (∝), and (♀) denote the data for samples F-2000, F-450, and F-128, respectively. Other symbols are the same as in Figure 1.

proportional to the actual relaxation time for the shear rate dependence of $\eta(\dot{\gamma})$.

Discussion

By using $\eta°$ and J_e data in good solvents obtained in the previous and present works and in a Θ solvent in the present work, τ_w was evaluated in good and Θ solvents and plotted in double-logarithmic forms against C in Figures 3 and 4, respectively. The concentration dependence of τ_w in a good solvent increases with decreasing molecular weight, while the increase is not clearly observed in the Θ solvent. From the molecular weight and concentration dependences of $\eta°$ and J_e in regions II and IV the following dependences of τ_w are expected:

In Region II ($C < C^{c-}$)

$$\tau_w \propto M^{4.4}C^{3.3} \quad \text{in good solvent} \quad (7a)$$

$$\tau_w \propto {}^{4.4}C^{5.8} \quad \text{in Θ solvent} \quad (7b)$$

In Region IV ($C > C_c{}^J$)

$$\tau_w \propto M^{3.4}C^{2.2} \quad \text{in good solvent} \quad (8a)$$

$$\tau_w \propto M^{3.4}C^{4.5} \quad \text{in Θ solvent} \quad (8b)$$

In Figure 5 double-logarithmic plots of $\tau_w/M^{4.4}$ and $\tau_w/M^{3.4}$ against C are shown for regions II and IV, respectively. The data points near $C_c{}^J$ are included in both regions. In both regions the data compose a single line for each solvent. The slopes of the lines in region IV and of the line for the data in good solvent in region II are equal to the exponents in eq 8 and 7a, respectively, while that for the data in Θ solvent in Region II is 5.1, which is slightly lower than the exponent in eq 7b. The discrepancy may be the experimental errors due to difficulty in measurements of $\eta°$ in Θ solvents, since the shear stresses observed are so small as to be close to the measurable limit of the rheogoniometer, in comparison with the stresses in good solvents. Unfortunately, the $\eta°$ data of polystyrene used for

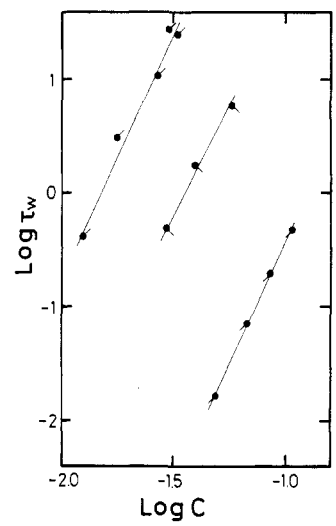

Figure 4. Concentration dependence of τ_w in Θ solvents. Symbols are the same as in Figure 1.

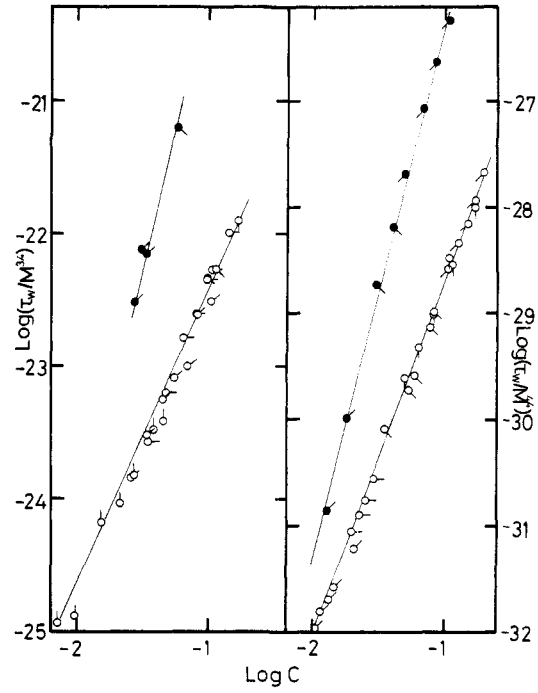

Figure 5. Double-logarithmic plots of $\tau_w/M^{4.4}$ (right side) and $\tau_w/M^{3.4}$ (left side) against C in the regions II and IV, respectively. Symbols are the same as in Figures 1 and 3.

evaluating τ_w deviate from the broken line determining the concentration dependence of $\eta°$ in opposite directions at the two lowest concentrations (♂) and the highest concentration (♃) in the Θ solvent, as can be seen in Figure 1. These facts cause the discrepancy in the exponent of τ_w in region II.

It should be noted that the data points are widely scattered if we plot all data in the form of log $(\tau_w/M^{3.4})$ versus log C as shown in Figure 6.

Figures 7 and 8 show the double-logarithmic plots of τ_0 against C in good and Θ solvents, respectively. In both figures the concentration dependences of τ_0 increase with decreasing molecular weight in the same way as in Figures 3 and 4.

In order to compare the molecular weight and concentration dependences of τ_0 with those of τ_w, we plot the τ_0 data in Figure 9 in the same way as τ_w in Figure 5. Here, the τ_w data in Figure 5 are shown by solid lines, and dotted lines are drawn parallel to the solid lines through the data

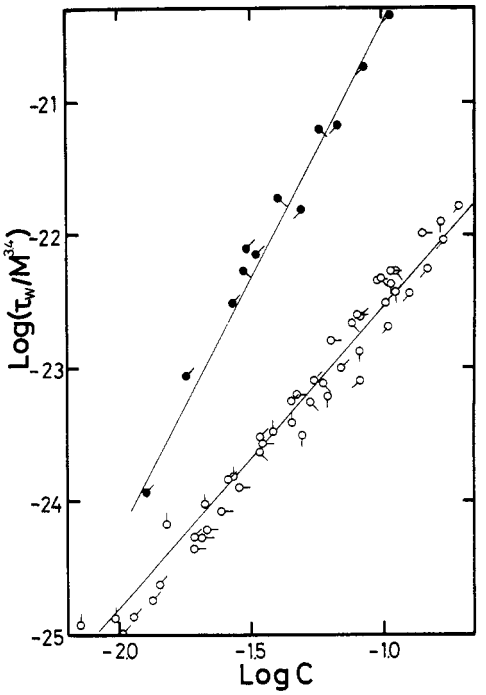

Figure 6. Double-logarithmic plots of $\tau_w/M^{3.4}$ versus C for all data in Figure 5.

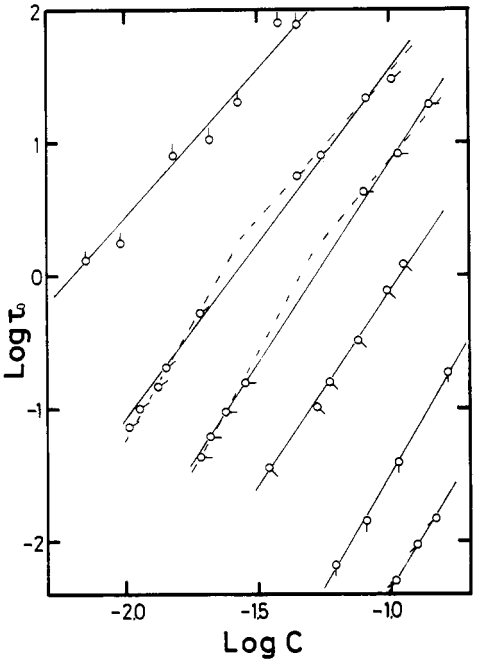

Figure 7. Double-logarithmic plots in τ_0 against C in good solvents. Symbols are the same as in Figure 3.

points of τ_0. Data of F-450 in region IV (♀) were evaluated by extrapolation of $\eta(\dot{\gamma})$ so that the experimental errors are larger than other data. Though the data in the good solvent are somewhat scattered in comparison with τ_w in Figure 5, it may be concluded that the molecular weight and concentration dependences of τ_0 are the same as those of τ_w.

Thus, the concentration dependences of τ_w and τ_0 are different in regions II and IV. Therefore, the concentration dependences of relaxation times for polymers with medium molecular weights in Figures 3 and 7 are understandable if we assume that the polymer solutions crossover from region II to IV with increasing the concentration, as shown by the two dotted lines for F 850 and 450 as examples in the figures.

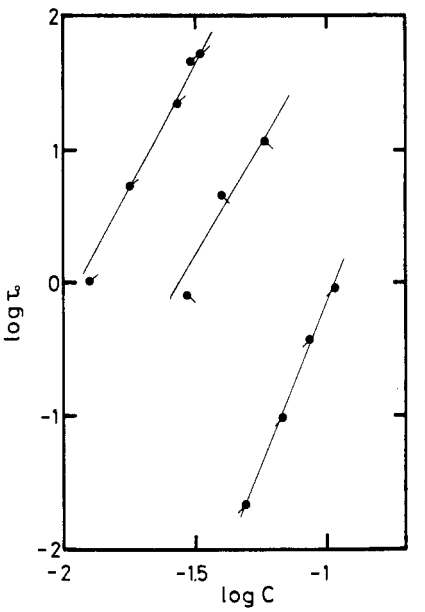

Figure 8. Double-logarithmic plots of τ_0 against C in Θ solvents. Symbols are the same as in Figure 1.

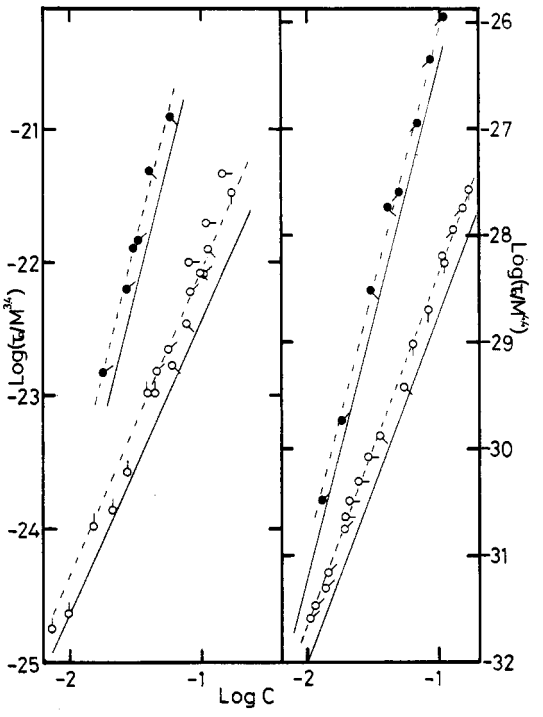

Figure 9. Double-logarithmic plots of $\tau_0/M^{4.4}$ and $\tau_0/M^{3.4}$ against C in regions II and IV, respectively. Symbols are the same as in Figures 1 and 3. Solid lines denote the data in Figure 5. Dotted lines are drawn parallel to the solid lines.

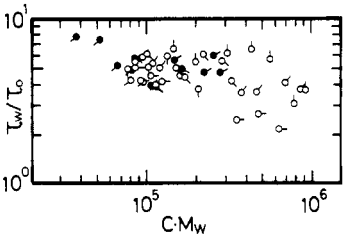

Figure 10. Double-logarithmic plots of τ_w/τ_0 against CM_w. Symbols are the same as in Figures 1 and 3.

Finally we directly compare τ_w with τ_0 over regions II and IV. Figure 10 shows double-logarithmic plots of the ratio of τ_w to τ_0 versus CM_w. The data are somewhat

scattered but it appears that the ratio decreases slightly with increasing CM_w. This result may imply that the ratio is somewhat different in different regions. However, if we consider that most of the ratio is almost constant in the range of 0.5 ± 0.2 (nearly equal to the value reported in the earlier work[14]) over wide ranges of concentration and molecular weight, we may conclude that there is no significant difference between dependences of τ_0 and τ_w on concentration, molecular weight, and solvent power over regions II and IV.

In highly entangled regions, τ_w or τ_0 is reported to be well represented by the longest relaxation times of the terminal relaxation process.[14] However, there are only a few studies on terminal relaxation processes in semidilute solutions.[18,19] Further work is needed to understand viscoelastic properties in semidilute solutions systematically.

Registry No. Polystyrene, 9003-53-6.

References and Notes

(1) Takahashi, Y.; Isono, Y.; Noda, I; Nagasawa, M. *Macromolecules* **1985**, *18*, 1002.
(2) Takahashi, Y.; Noda, I.; Nagasawa, M. *Macromolecules* **1985**, *18*, 2220.
(3) de Gennes, P.-G. *Macromolecules* **1976**, *9*, 594.
(4) de Gennes, P.-G. *Scaling Concepts in Polymer Physics*; Cornell University Press: Ithaca, NY, 1979; Chapter 8.
(5) Graessley, W. W. *Adv. Polym. Sci.* **1974**, *16*, 25.
(6) Ferry, J. D. *Viscoelastic Properties of Polymers*, 3rd ed.; Wiley: New York, 1980; Chapters 3, 10.
(7) Graessley, W. W. *Polymer* **1980**, *20*, 258.
(8) Noda, I.; Higo, Y.; Ueno, N.; Fujimoto, T. *Macromolecules* **1984**, *17*, 1055.
(9) Graessley, W. W.; Hazleton, R. L.; Lindeman, L. R. *Tran. Soc. Rheol.* **1967**, *11*, 267.
(10) Endo, H.; Fujimoto, T.; Nagasawa, M. *J. Polym. Sci., Polym. Phys. Ed.* **1971**, *9*, 345.
(11) Sakai, M.; Fujimoto, T.; Nagasawa, M. *Macromolecules* **1972**, *5*, 786.
(12) Berry, G. C.; Hager, B. L.; Wong, C. P. *Macromolecules* **1977**, *10*, 361.
(13) Isono, Y.; Nagasawa, M. *Macromolecules* **1980**, *13*, 862.
(14) Graessley, W. W. *Adv. Polym. Sci.* **1974**, *16*, Ch 8.
(15) Isono, Y.; Fujimoto, T.; Kajiura, H.; Nagasawa, M. *Polym. J. (Tokyo)* **1980**, *12*, 363.
(16) Endo, H.; Nagasawa, M. *J. Polym. Sci., Polym. Phys. Ed.* **1970**, *8*, 371.
(17) Kajiura, H.; Endo, H.; Nagasawa, M. *J. Polym. Sci., Polym. Phys. Ed.* **1973**, *11*, 2371.
(18) Osaki, K.; Nishizawa, K.; Kurata, M. *Macromolecules* **1982**, *15*, 1068.
(19) Osaki, K.; Nishimura, Y.; Kurata, M. *Macromolecules* **1985**, *18*, 1153.

Incorporation of Molecular Orientation into Systems of Lamellar Morphology. 1. Effects of Packing Entropy on the Lamellar Thickness of Block Copolymers

E. A. DiMarzio

National Bureau of Standards, Gaithersburg, Maryland 20899. *Received June 29, 1987; Revised Manuscript Received January 23, 1988*

ABSTRACT: Equations for the dimensions of the A and B regions of monodisperse diblock copolymers with lamellar morphology are obtained. An important feature of the treatment is the incorporation of the orientation-dependent packing entropy into the formalism. The equations are believed to be accurate over the whole range of orientation of bonds, from random orientation to perfect alignment. Copolymer thicknesses vary as the $^2/_3$ power of molecular weight to the first power depending on the amount of orientation induced by the packing entropy and the energetics. The amount of bond orientation in stretched molecules in bulk material is twice what the molecules would have if they were stretched (by the same stretch ratio) in solvent. It is observed that this effect is important to those systems of micelles, vesicles, membranes, soaps, liquid crystals, and block copolymers that experimentally are known to display significant orientation, and it is suggested that extant theories can be modified to include the effect.

1. Introduction

This paper is concerned mainly with the effect of orientation of polymer bonds on the thermodynamics of monodisperse block copolymers. A simple calculation given previously[1] shows that the dimensions of the homopolymer portions in the direction perpendicular to the lamellar surfaces vary as the $^2/_3$ power of the molecular weight. This means that the bonds have a net preferential orientation in the perpendicular direction. It is meaningful to ask how this orientation affects the thermodynamics of such systems.

Previous theories of block copolymers do not predict significant orientation. However, these theories do not take into account the orientation-dependent packing entropy, which when properly treated leads to the liquid crystal phase[2-5] (and also substantial orientation of the polymer) if the molecules are stiffer than a critical value. That this effect is relevant to block copolymers is suggested by those few existing experiments that show that the shape of small molecules dissolved in the lamella is nonspherical even though these molecules are small compared to the thickness of the lamella in which they are imbedded.[6] Presumably these small molecules sense the background grain of larger molecules comprising the lamella. This is consistent with the observation that nematic liquid crystals orient dissolved η-alkanes.[7]

Another reason for believing that the orientation effects are important is the existence of liquidlike theories of rubber elasticity that allow for competition for space among chains touching each other in a bulk rubber.[8,9] These theories predict a significant contribution to the stress–strain relation arising from the packing entropy.

The third reason for treating orientation effects is that they are known to be important in membranes. Not only is the amount of bond orientation substantial, but also it is strongly dependent on the location of the bond in the lipid molecules.[10]

Although we will develop our equations in the context of a discussion of block copolymers, the treatment will have application also to membranes, soaps, and smectic liquid